Contents lists available at SciVerse ScienceDirect

Journal of Steroid Biochemistry and Molecular Biology

Review

Modulation of synaptic plasticity in the hippocampus by hippocampus-derived estrogen and androgen ☆

Yuuki Ooishi [a], Suguru Kawato [a,b,c,d,*], Yasushi Hojo [a,b,c], Yusuke Hatanaka [a], Shimpei Higo [a], Gen Murakami [a,c], Yoshimasa Komatsuzaki [a], Mari Ogiue-Ikeda [a,d], Tetsuya Kimoto [a], Hideo Mukai [a,b,c]

[a] Department of Biophysics and Life Sciences, Graduate School of Arts and Sciences, The University of Tokyo, 3-8-1 Komaba, Meguro, Tokyo 153-8902, Japan
[b] Core Research for Evolutional Science and Technology Project of Japan Science and Technology Agency, The University of Tokyo, Japan
[c] Bioinformatics Project of Japan Science and Technology Agency, The University of Tokyo, Japan
[d] Project of Special Coordinate Funds for Promoting Science and Technology, The University of Tokyo, Japan

ARTICLE INFO

ABSTRACT

The hippocampus synthesizes estrogen and androgen in addition to the circulating sex steroids. Synaptic modulation by hippocampus-derived estrogen or androgen is essential to maintain healthy memory processes. Rapid actions (1–2 h) of 17β-estradiol (17β-E2) occur via synapse-localized receptors (ERα or ERβ), while slow genomic E2 actions (6–48 h) occur via classical nuclear receptors (ERα or ERβ). The long-term potentiation (LTP), induced by strong tetanus or theta-burst stimulation, is not further enhanced by E2 perfusion in adult rats. Interestingly, E2 perfusion can rescue corticosterone (stress hormone)-induced suppression of LTP. The long-term depression is modulated rapidly by E2 perfusion. Elevation of the E2 concentration changes rapidly the density and head structure of spines in neurons. ERα, but not ERβ, drives this enhancement of spinogenesis. Kinase networks are involved downstream of ERα. Testosterone (T) or dihydrotestosterone (DHT) also rapidly modulates spinogenesis. Newly developed Spiso-3D mathematical analysis is used to distinguish these complex effects by sex steroids and kinases.

It has been doubted that the level of hippocampus-derived estrogen and androgen may not be high enough to modulate synaptic plasticity. Determination of the accurate concentration of E2, T or DHT in the hippocampus is enabled by mass-spectrometric analysis in combination with new steroid-derivatization methods. The E2 level in the hippocampus is approximately 8 nM for the male and 0.5–2 nM for the female, which is much higher than that in circulation. The level of T and DHT is also higher than that in circulation. Taken together, hippocampus-derived E2, T, and DHT play a major role in modulation of synaptic plasticity.

Contents

1. Introduction

Occurrence of local synthesis of estrogen and androgen in the adult hippocampus supports estrogen-dependent regulation of memory processes which occur rapidly [1–5]. Different from circadian rhythm-dependent synthesis that occurs in ovary or testis, synaptic synthesis (transient and rapid) of estrogen and androgen could occur dependent on synaptic events including long-term potentiation (LTP) and long-term depression (LTD) [1–5].

Not only electrophysiological properties but also dendritic spines have been studied in relation to memory processes and synaptic plasticity which are regulated by neurotransmitters, because synapse is a site of memory storage and spine is a post-synaptic structure.

For decades, neuromodulatory actions of gonadal sex hormones have been extensively investigated, because circulating sex hormones can penetrate into the hippocampus by crossing the blood–brain barrier. Genomic slow modulation of synaptogenesis or electrophysiological properties is investigated by estrogen replacement for ovariectomized female rats [6–11]. An increase of synapses or an enhancement of synaptic transmission is observed upon estrogen replacement of ovariectomized animals. Genomic slow modulation of spines is also observed in slice cultures [6–11]. These slow genomic effects are mediated via nuclear estrogen receptors ERα/ERβ which initiate transcription processes. The slow/genomical modulation of NR2B by 17β-estradiol (E2) replacement enhances LTP in ovariectomized rat [12,13].

The acute/rapid effect of E2 (within 1–2 h) also occurs by modulating spine density or synaptic transmission of the hippocampal slices [6,7,14–17]. Acute modulation of synapses by E2 occurs via synaptic ERα/ERβ which drives kinases in their downstream [16,18]. Since kinases not only work within synapses but also move into nuclei to drive gene transcription, acute E2 effects also drive genomic processes which may slowly enhance synaptic contacts.

These acute modulations, relating to memory formation processes, favor locally synthesized steroids rather than circulating gonadal hormones which travel a long distance before reaching the brain. Rather than being a limiting factor, a weak activity of sex steroid production in the hippocampus is sufficient for the local usage within small volume of neurons (i.e., an intracrine system). This intracrine system contrasts with the endocrine organs in which high expression levels of steroidogenic enzymes are necessary to supply steroids to many other organs via the blood circulation. For hippocampus-derived sex hormones, one of the essential functions may be the rapid and repetitive modulation of synaptic plasticity and cognitive functions, in addition to genomic slow modulation.

2. Modulation of synaptic plasticity by hippocampal sex steroids

2.1. Modulation of long-term potentiation (LTP) and long-term depression (LTD)

Nanomolar level of E2 exerts an acute influence (0.5–1 h) on the synaptic transmission of hippocampal slices, as demonstrated by electrophysiological investigations.

Interestingly, the effects of E2 on the basal excitatory post-synaptic potential (EPSP) or LTP may strongly depend on the age of rats. In the hippocampus from 4- to 6-week-old or 200 to 350 g (approx. 6–8 week-old) Sprague-Dawley rats, perfusion of 1–10 nM E2 rapidly increases the basal EPSP (thereby enhances LTP) at CA3–CA1 synapses [6,7,19]. Concerning 4 week-old Wistar rats, we sometimes (less than 20% probability) observed the rapid basal EPSP elevation upon E2 perfusion [14,20,21]. On the other hand 1–10 nM E2 did not affect the basal EPSP and LTP in the hippocampus from 12 week-old (3 month-old) adult Wistar rats [16,20,22]. No rapid basal EPSP elevation upon E2 perfusion is also observed in case of 3–5 month-old as well as 18–24 month-old Sprague-Dauley rats [23]. Therefore, E2 may have significant effects on the basal EPSP of younger rats (4–8 weeks old) and may not have effect on older adult rats (12 weeks-old or elder). In 3–4 week-old (early puberty) rats, E2 even suppresses LTP-induction down to the similar level to that of 12 week-old rats [9,22]. In these investigations, high-frequency tetanic stimulation (1 s) is used for LTP-induction, in which the phosphorylation of α-amino-3-hydroxy-5-methylisoxazole-4-propionic acid (AMPA) receptors by CaM kinase II is a dominant process at high Ca^{2+} concentration (approx. 10 μM). E2 may not play an important role on the LTP-induction processes during tetanic stimulation.

Stress is known to suppress the function of the hippocampus. "Can E2 induce neuroprotective effects on synaptic transmission during acute stress?" may be more interesting topic than E2 alone effects. Stressful level of corticosterone (CORT) at 1 μM induces rapid suppression of LTP at CA3–CA1 synapses. Upon perfusion of 1 nM E2, LTP-suppression by CORT was abolished (Fig. 1) [24]. N-methyl-D-aspartate (NMDA) receptor-derived EPSP was used to analyze the mechanisms of these events. E2 abolished CORT-induced suppression of NMDA-R-EPSP (Fig. 1). This CORT-induced suppression was abolished by calcineurin inhibitor, and the rescue effect by E2 on the CORT-induced suppression was inhibited by Erk MAP kinase inhibitor. The CORT-induced suppressions of LTP and NMDA-R-EPSP were abolished by glucocorticoid receptor (GR) antagonist, and the restorative effects by E2 on these processes were mimicked by ERα and ERβ agonists. Taken together, E2 rapidly rescues LTP and NMDA-R-EPSP from CORT-induced suppressions. Synaptic GR (see Fig. 6E) → calcineurin pathway is involved in these suppressive effects. The rescue effects by estradiol are driven via synaptic ERα or ERβ → Erk MAP kinase pathway, probably induces activation of NMDA receptor by phosphorylation of NR2B → rescue of Ca^{2+} influx from CORT-induced suppression during tetanic stimulation → restoration of phosphorylation of AMPA receptor → LTP restoration (Fig. 2) [24]. Note that synaptically localized GR, ERα were observed by immunoelectron microscopic analysis (Fig. 6) [16,25]. Under these conditions of weakend LTP by CORT, ERα may play significant role due to lower Ca^{2+} concentration (may be 5 μM).

In memory processing, not only LTP (memory forming mechanism) but also LTD (memory erasing mechanism) are essential. Mutant mice, which show enhanced LTP and suppressed LTD, have shown impaired learning of the Morris water maze [26]. This suggests that LTD may be required to "correct" wrong memories formed by some LTP processes, which store not only correct information but also incorrect information. We found that LTD was rapidly enhanced by a 1–10 nM E2 perfusion (for 1 h) in hippocampal slices from adult rats (Fig. 3) [16,20]. Recordings are performed using custom multielectrodes. LTD can be induced
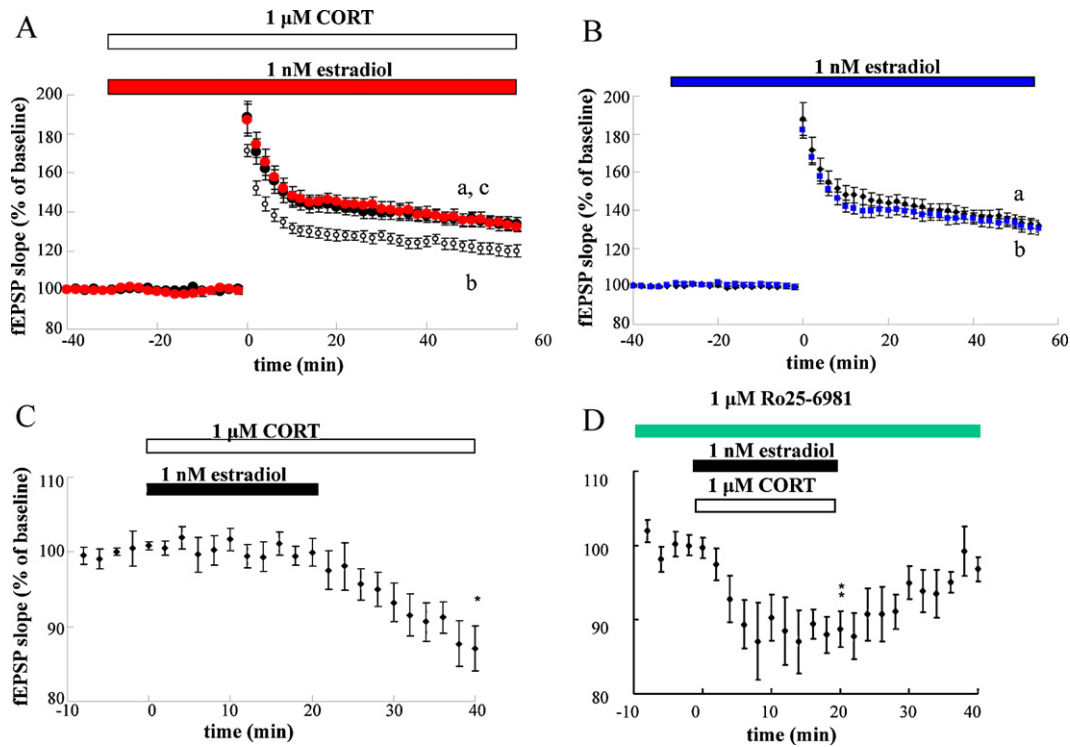
Fig. 1. Estradiol (E2) rapidly rescues LTP from CORT-induced suppression in 12 week-old male hippocampus. (A) One micromolar CORT suppresses LTP and 1 nM E2 rescued LTP from the CORT-induced suppression at CA3–CA1 synapses of acute slices. Curve a, control slices (black closed circle); curve b, 1 μM CORT treated slices (open circle); curve c, slices treated by 1 μM CORT plus 1 nM E2 (red closed circle). Illustrated data points and error bars represent the mean ± SEM. Note that co-perfusion of RU486 (GR inhibitor) with CORT abolished the CORT-induced suppression of LTP. Vertical axis indicates the maximal EPSP slope. Baseline is set at 100%. Open bar above the graph indicates the period of time during which CORT was administered. Red closed bar above the graph indicates the period of time during which E2 was administered. (B) One nanomolar estradiol alone does not affect LTP at all at CA3–CA1 synapses of acute slices. Curve a, control (black closed circle), curve b, 1 nM E2 (blue closed square). (C) E2 rescued NMDA-receptor-derived EPSP slope from the CORT-induced suppression. Time dependence of NMDA-R-EPSP slope is shown for 20 min. Rapid abolition of the CORT-induced suppression occurs by 1 nM E2 perfusion. The period of CORT perfusion is indicated by the open bar, and that of E2 perfusion by the closed bar. (D) Abolition of the E2-induced rescue effect on CORT-induced suppression of NMDA-R-EPSP slope following the perfusion of 1 μM Ro25-6981, an NR2B inhibitor (perfused as indicated by the green bar). Statistical significance (*$p < 0.05$; **$p < 0.01$). (For interpretation of the references to color in this figure legend, the reader is referred to the web version of the article.)

Modified from [24].
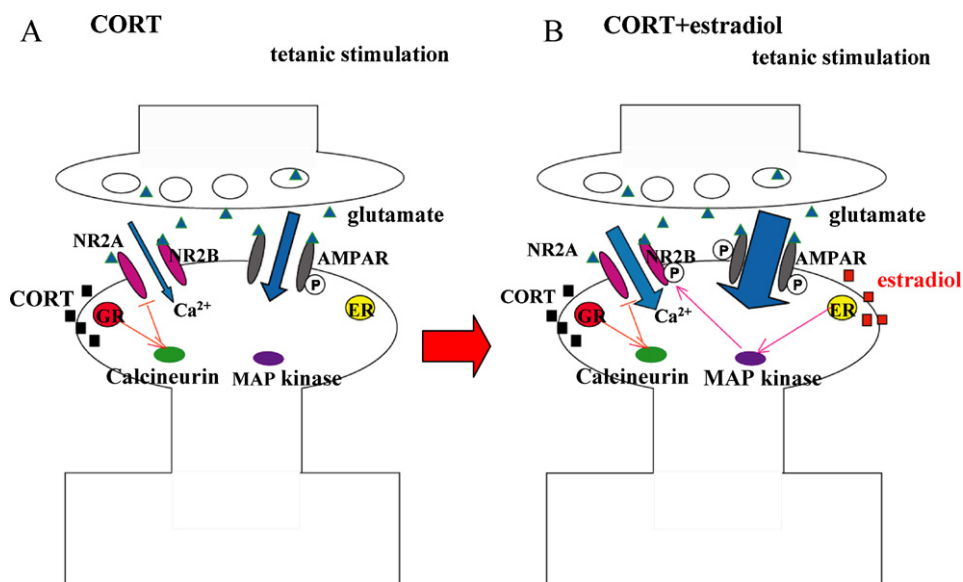
Fig. 2. Hypothetical mechanisms of modulation of LTP by CORT and E2. (A) CORT-induced LTP suppression. An application of 1 μM CORT drives the following signaling pathway: CORT → GR → calcineurin → dephosphorylation of NMDA receptor subunit NR2A. Upon tetanic stimulation, AMPA receptor (AMPAR) is not sufficiently phosphorylated at the residue of serine 831, because CORT already suppressed NMDA receptor (NMDAR)-derived Ca^{2+} current by dephosphorylation of NR2A, resulting in the suppression of LTP-induction. (B) Rescue by E2 of LTP from CORT-induced suppression. The application of 1 nM E2 drives the following signaling pathway: E2 → ERα or ERβ → Erk MAP kinase → NR2B phosphorylation. E2 finally phosphorylates an NMDA receptor subunit NR2B. Upon tetanic stimulation, estradiol-induced restoration of NMDAR derived Ca^{2+} current by phosphorylation of NR2B causes sufficient phosphorylation of AMPAR at the residue of serine 831, resulting in the restoration of LTP-induction.

Modified from [24].
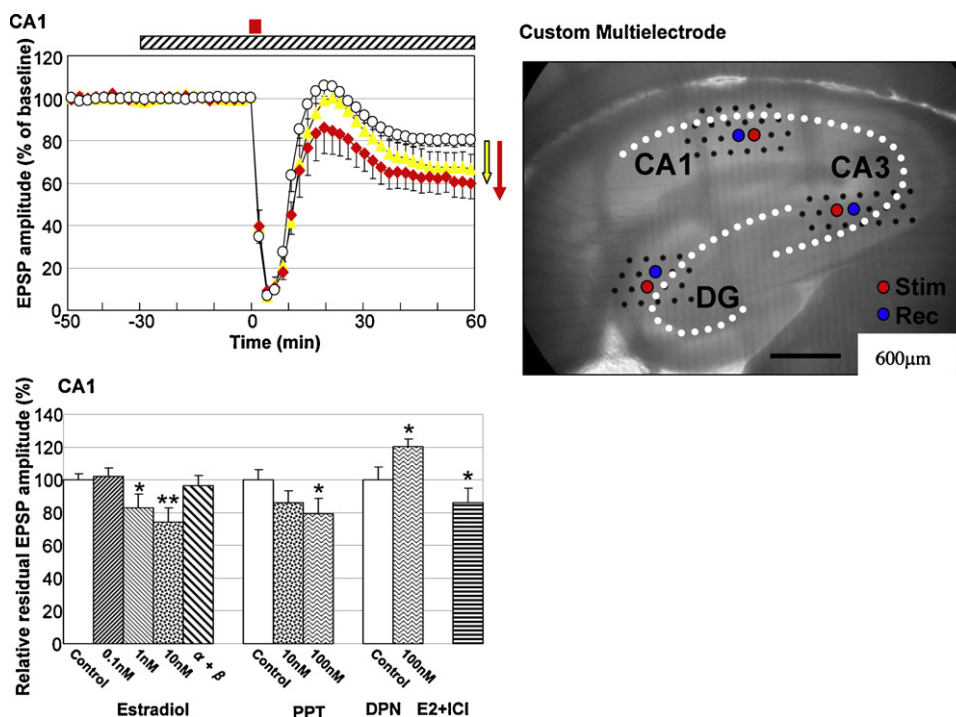
Fig. 3. Rapid estrogen modulation of LTD (adult male rat). [Upper left] Time dependence of maximal EPSP amplitude in CA1 of hippocampal slices. E2 concentration was 0 nM (open circle), 1 nM (yellow closed triangle) and 10 nM (red closed diamond), respectively. Here, 100% EPSP amplitude refers to the EPSP value at $t = -40$ min prior to NMDA stimulation, irrespective of the test condition. LTD was induced by 30 μM NMDA perfusion at time $t = 0$–3 min (closed red bar above the graph). Hatched bar above the graph indicates the E2 administration period. [Upper right] Custom-made 64 multielectrode probe (MED64, Panasonic, Japan) with the hippocampal slice. Stimulation (red circle) and recording (blue circle) electrodes are indicated. [Lower left] Comparison of modulatory effect on LTD by E2 and agonists in the CA1 of hippocampal slices. Vertical axis represents relative EPSP amplitude at $t = 60$ min, where EPSP amplitude at $t = 60$ min of the control slice without drug application is taken as 100%. From left to right, 17β-E2 (E2), PPT (ERα agonist) and DPN (ERβ agonist) at indicated concentrations. Co-perfusion of 10 nM 17α-E2 with 1 nM 17β-E2 ($\alpha + \beta$) blocks the 17β-E2 effect of LTD enhancement. Co-perfusion of 1 μM ICI with 10 nM 17β-E2 did not suppress the enhancing effect of LTD by estradiol. Importantly, ICI does not inhibit any type of E2 effects on electrophysiological signals, such as LTP, LTD or kainate current presented in previous reports [16,20,60]. The ICI results suggest that dimer formation of ERα/ERβ is not involved in the E2-modulation of synaptic transmission. An NMDA-induced chemical LTD is used for adult hippocampal slices, because an electrical LTD is not inducible for adult hippocampal slices. In contrast, an electrical LTD is inducible for younger hippocampus which is younger than 3 week-old. The significance of the estradiol effect was confirmed at 60 min via statistical analysis (*$p < 0.05$; **$p < 0.01$). (For interpretation of the references to color in this figure legend, the reader is referred to the web version of the article.)

Modified from Mukai et al. [16].

pharmacologically by the transient application of NMDA. This LTD is induced by the activation of phosphatase due to a moderate Ca^{2+} influx through NMDA receptors [27]. Note that LTD is effectively induced by the transient application of NMDA (chemical LTD) for adult hippocampus, whereas low frequency electrical stimulation cannot induce LTD in adult slices. Low frequency electrical stimulation can induce LTD in slices from rats younger than 4 weeks of age. A 30 min perfusion of 10 nM E2 significantly enhances LTD resulting in a decrease in plateau EPSP amplitude (at 60 min after NMDA application), for example, 80% → 60% (CA3–CA1 synapses) [16,20]. Investigations using specific estrogen agonists indicated that the contribution of ERα but not ERβ is essential for these E2 effects. ERα agonist exhibits a significant LTD enhancement in CA1, while ERβ agonist induces a suppression of LTD in CA1, implying that the contribution of ERβ is opposite to that of ERα in the E2 effect on LTD. Taken collectively, E2-bound ERα may activate phosphatase at the moderate Ca^{2+} concentration of 0.7–1 μM induced upon 30 μM NMDA application [28], and facilitate dephosphorylation of AMPA receptors resulting in the enhancement of LTD.

On the other hand, E2-bound ERα is not functional in LTP modulation at the transiently high Ca^{2+} concentration of approx. 5–12 μM under tetanic stimulation [20,28–30], because the phosphorylation of AMPA receptors by CaM kinase II is the dominant process at the high Ca^{2+} concentration.

E2-induced rapid modulation of LTD or LTP occurs only in pre-existent synapses, because newly generated spines induced by

E2-treatments do not form new synapses within 2 h, as judged from no increase in the baseline magnitude of EPSP signal during 2 h of E2 perfusion [16]. On the other hand, the slow effect of E2 (2–4 days) enhances LTP via formation of new synaptic contacts for estrogen supplemented ovariectomized 8-week female rats [12,31]. The electrophysiological properties of NMDA receptor-mediated transmission are altered by estrogens [32].

2.2. Spinogenesis

Dendritic spines (presynaptic structures) can be rapidly modulated by E2 [33]. Spines consist of not only spine-synapses (spines which form synapses, approx. half of spines) but also free spines (spines without forming synapses, approx. half of spines). Modulation of spinogenesis involves the production of new spines that create sites for new neuronal contacts. Spines are rapidly modulated upon E2 application, which is observed by single spine analysis of Lucifer-Yellow injected neurons in hippocampal slices from adult male rats (3 months) [17,30,34,35]. Following a 2 h treatment with 1 nM E2 in the stratum radiatum of the CA1 region, the total density of spines significantly increases from 0.85 spines/μm to 1.31 spines/μm (Fig. 4) [16]. ERα agonist propyl-pyrazole-trinyl-phenol (PPT) [36] also induces a significant enhancement of the spine density to 1.20 spines/μm. However, ERβ agonist, diaryl-propionitrile (DPN) [36], increases the spine density only slightly. Blocking ERs by ICI 182,780 completely suppresses the enhancing
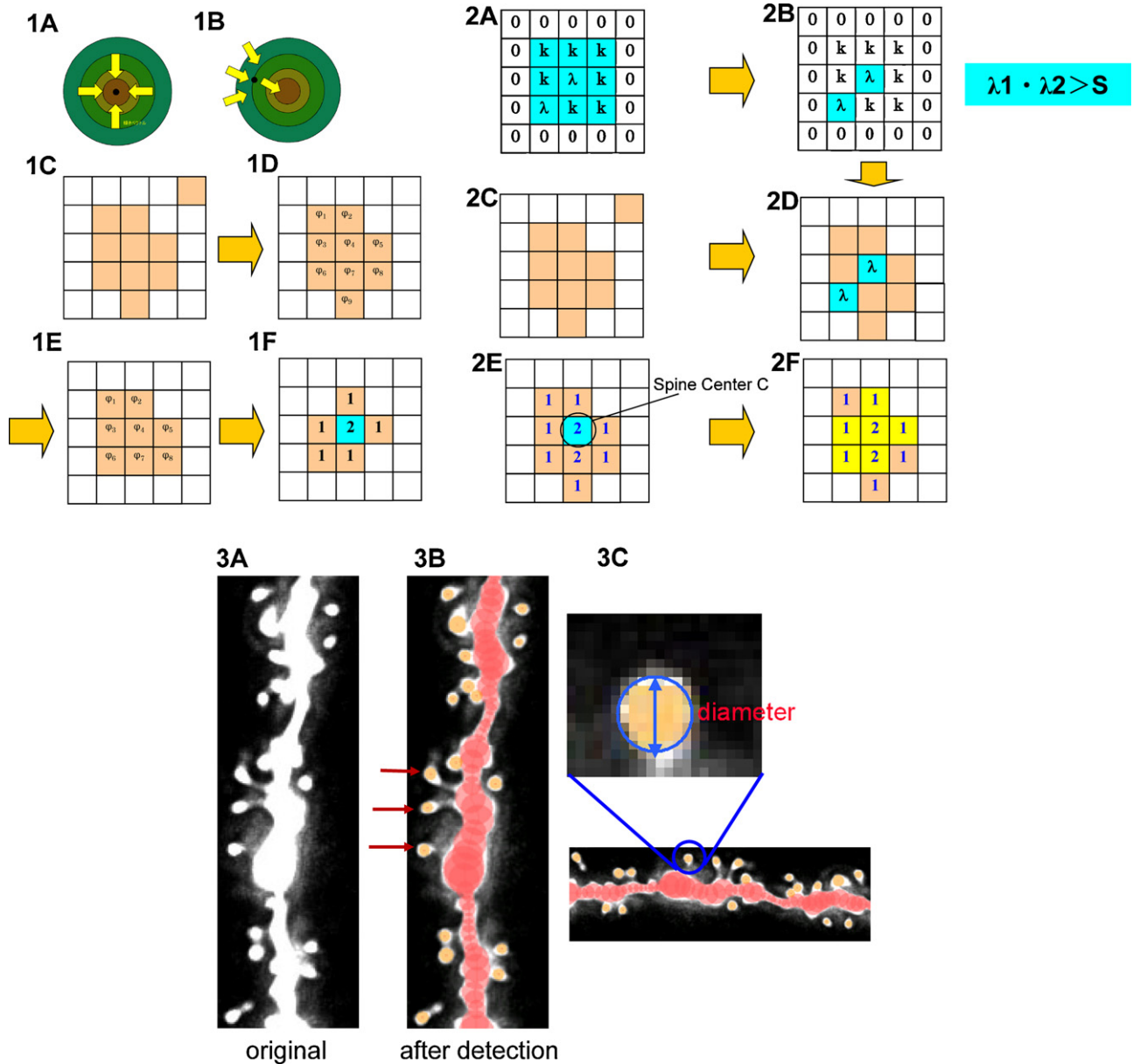
Fig. 4. Flow of spine head diameter determination by Spiso-3D. We use the spine brightness function $I_A(\mathbf{x}_1)$ which is obtained by subtraction of traced dendrite from the total brightness function. The spine head region points are extracted as points where both λ_1 and λ_2 yield negative values (1D and 2A), since the spine head is an isolated closed volume with a closed surface. (1) Locating spine center at an optical slice with $z = z_j$. (1A) A schematic illustration of the pixel $P(x,y)$ that is a true spine center. Four nearest neighbors in X or Y direction with all ϕ_A are negative. (1B) $P(x,y)$ that is not a true spine center with one positive ϕ_A. (1C) A schematic example of gradient vector image. Painted tiles indicate pixels of spine center candidate, i.e. $||grad\,\phi_A|| > 0$, white tiles are pixels with $grad\,\phi_A = 0$. (1D) Calculation of the inner product of gradient vectors ϕ at pixels where λ_1 and λ_2 are both negative. (1E) Spine center detection image created by selecting pixels with negative ϕ_A. (1F) Digitized spine center detection image. In spine center candidates, minimum number of pixels to reach the center pixel from perimeter (edge) pixel is counted and assigned on each pixel. A perimeter pixel has a value of 1. The pixel having maximum number $r_c = 2$ is of the spine center C. (2) Spine diameter determination. Determination of spine head diameter is performed using the "distance image" that is the digitized "radius detection image". (2A) Spine center detection image. Eigenvalues of Hessian matrix are calculated at each pixel. "λ" indicates a pixel where (1) eigenvalues λ_1 and λ_2 are both negative and (2) $\lambda_1\lambda_2 > S$ (S: sensitivity set in the Spiso program by user). "k" indicates pixel with $\lambda_1\lambda_2 \leq S$. (2B) Image of information of spines. "λ" pixels are marked for spine center candidates, while "k" pixels are omitted. (2C) Gradient vector image in (1C). (2D) By superimposing (2B) and (2C), the connected area in gradient vector image with "λ" pixel inside is defined as "spine". The spine pixels are indicated as orange pixels. (2E) The radius detection image. To create the digitized distance image, the minimum number of pixels to reach the center pixel from the perimeter pixel is assigned on each pixel. (2F) Spine diameter is determined by combining the spine center detection image (1F) with (2E), by superimposing both center C. The combined area is again digitized to create the distance image. The maximum distance number R (assigned for the center C) is adopted as a spine radius (a spine diameter $D_j = 2R$). Finally, 3-dimensional integration of spines is performed, resulting in determination of maximum D_j as the spine diameter D. (3) Results of calculated dendritic spines by Spiso-3D. (3A) Original image of dendrite. (3B) Traced dendrite (connected series of red circles) and spines (yellow circles) superimposed on the image. (3C) Calculated diameters of spines are superimposed on the spine images. (For interpretation of the references to color in this figure legend, the reader is referred to the web version of the article.)

Modified from Mukai et al. [38].

effect of E2 on the spine density. Interestingly, blocking ERK MAP kinase by PD98059 or U0126 completely prevents the E2-induced spinogenesis [35]. Taken together, the rapid E2-induced enhancement of the CA1 spine density probably occurs by the activation of Erk MAP kinase via ERα [37]. It should be noted that when the Ca^{2+} concentration in spines is decreased from the basal level by blocking NMDA receptors with MK-801, the enhancing effect by E2 is completely suppressed. The function of E2-bound ERα probably requires the basal Ca^{2+} level of approximately 0.1–0.2 nM.

Comparison with the total density of spines is facile and useful, however in many cases the total spine density is not sensitive for discrimination of different steroid treatments. For example the effects of E2, T and DHT on the total spine density are indistinguishable. In such a case, closer examination of spine head diameter distribution is necessary in order to differentiate between T, DHT and E2 treatments. A rigorous analysis of spine morphology is necessary.

In adult hippocampal slices, the majority of spines (>95%) have distinct heads and necks, while the populations of stubby spines (approx. 5%, no neck) and filopodium (approx. 1%, no head) are very small. Therefore, the determination of spine head diameter distribution is a very powerful method in order to analyze the complex morphological changes in spines, instead of the conventional classification of mushroom/thin/stubby/filopodium [30].

To do a rigorous spine head diameter analysis, we have developed Spiso-3D software which mathematically and automatically identifies the spine head and determines the diameter of the spine from their geometrical features (see Fig. 4-1, -2, -3, flow chart images of calculation) [38]. The identification of the spine head is performed by extraction of spine head points within a closed surface. For mathematical analysis, we use Hessian tensor that is obtained as 2nd derivatives from Taylor expansion of the spine brightness function $I(\mathbf{x})$ in each optical slice, in 20–30 z-series optical slices obtained by confocal images:

$$I(\mathbf{x} + \varepsilon\mathbf{u}) = I(\mathbf{x}) + \varepsilon I'(\mathbf{u}) + \frac{1}{2}\varepsilon^2 I''(\mathbf{u}) + \cdots$$

$$= I(\mathbf{x}) + \varepsilon \cdot grad\, I \cdot \mathbf{u} + \frac{1}{2}\varepsilon^2 \mathbf{u}^t \mathbf{H}\mathbf{u+} = I(\mathbf{x}+\varepsilon\mathbf{u})$$

$$= I(\mathbf{x}) + \varepsilon(g_1 u_1 + g_2 u_2) + \frac{1}{2}\varepsilon^2(\lambda_1 u_1^2 + \lambda_2 u_2^2)+$$

with

$$grad\, I = \begin{pmatrix} \frac{\partial I}{\partial x} \\ \frac{\partial I}{\partial y} \end{pmatrix}, \quad H = \begin{pmatrix} \frac{\partial^2 I}{\partial x^2} & \frac{\partial^2 I}{\partial x \partial y} \\ \frac{\partial^2 I}{\partial y \partial x} & \frac{\partial^2 I}{\partial y^2} \end{pmatrix}, \quad diag\, H = \begin{pmatrix} \lambda_1 & 0 \\ 0 & \lambda_2 \end{pmatrix}$$

where λ_1 and λ_2 are the eigenvalues of Hessian tensor. Spiso-3D extracts spines based on geometrical features of spines, therefore completely different approach from other methods including the ray-bursting method [39,40] that exploits information of brightness to define boundaries of spines. Results obtained by Spiso-3D are almost identical to those by Neurolucida (MicroBrightFeild, USA, manual-based analysis software) [38]. For quantitative comparison, we classify spines into three subclasses, i.e., small-head spines (0.2–0.4 μm), middle-head spines (0.4–0.5 μm) and large-head spine (0.5–1.0 μm).

Using Spiso-3D, we clearly distinguished the different effects of testosterone (T, 10 nM), dihydrotestosterone (DHT, 10 nM) and E2 (1 nM) on hippocampal spines in CA1 pyramidal neurons in acute hippocampal slices (Fig. 4). These sex-hormones rapidly (within 2 h) increased the total spine density from 0.97 spines/μm to 1.28 (T), 1.32 (DHT) and 1.34 (E2), respectively. While the effects of T, DHT and E2 treatment on the total spine density

were indistinguishable, closer examination spine head diameter revealed marked differences in the distribution of spine head diameter between T, DHT and E2 treatments. DHT treatment was found to increase large- and middle-head spines, whereas T increased large- and small-head spines (Fig. 5). In contrast, E2 treatment increased only small-head spines. The observed differences in the effects of the hormones on spine subpopulations may have functional implications, for example, large-head spines may contain more AMPA receptors, since spine-head size positively correlates with the density of AMPA-type glutamate receptors [41,42]. Since the induction of long-term potentiation (LTP) is dependent on the density of AMPA receptors in spines [41,42], increased density of AMPA receptors in large-head spines could facilitate LTP. Increased density of large-head spines following DHT treatments could potentially facilitate LTP induction, in contrast to T, which only moderately increased large-head spines, or E2 which had no effect on the density of large-head spines. These findings demonstrate the importance of the consideration of spine diameter to distinguish different types of neurotrophic effects of estrogen and androgen.

Attention must be paid to 'acute' hippocampal slices often used for in vitro investigations of spinogenesis or LTP/LTD. Steroids are depleted in 'acute' slices during recovery incubation in steroid-free ACSF for 1–2 h, in order to remove damaged surface cells which were damaged by vibratome slicing (Fig. 9-2). Because the concentration of E2, T and DHT is less than 0.5 nM in acute slices, supplementation of E2, T or DHT (1–10 nM) induces significant effects [6,7,9,16,22,43]. In this sense, these 'acute' slice experiments may represent an in vitro model of in vivo estrogen replacement therapy in which circulating estrogen-depleted ovariectomized female rats (hippocampal E2 of 0.2 nM) are injected with E2 at 10–50 μg/kg rat weight. Probably E2 (1–10 nM) cannot induce any effect in cultured slices which keep endogenous 5–10 nM E2 level. On the other hand, the hippocampus in vivo contains 5–10 nM E2, T and DHT, preventing action of such a nanomolar E2, T and DHT.

The rapid effect of estrogen is also observed in vivo. Leranth and co-workers demonstrate that the E2 (60 μg/kg) rapidly (∼30 min) increases the spine-synapse density due to synaptic rearrangements in ovariectomized adult rats after E2 injection, using electron micrographic analysis [44]. On the other hand, the slow genomic effects (1–4 days) of E2 on spine plasticity have been extensively investigated in vivo from the view point of estrogen replacement therapy. For example, a supplement of estrogen to ovariectomized adult female rats increase the density of spines in the stratum radiatum of CA1 pyramidal neurons, resulting in a recovery of spines to the level of intact rat [44–47]. These enhancement effects on spinogenesis are also observed as rapidly as 4 h after s.c. injection of estrogen [44]. Results from in vivo investigations of rats may reflect not only the direct but also the indirect effects of E2 on glutamatergic neurons via cholinergic or serotonergic neurons, projecting to the hippocampus [44,48]. Estrogen mediates slow spine changes by means of NMDA receptors. Estradiol increases the binding of NMDA agonist, as well as the NR1 subunit levels in CA1 neurons [49,50]. Estrogen-induced increases in spine density are blocked by NMDA receptor antagonists [11,51].

In vitro investigations also show that the CA1 spine density increases following several days' treatment of cultured hippocampal slices with 0.5 μM (=0.2 μg/mL) exogenous E2 [8]. The contribution of hippocampus-derived E2 has been examined by Rune and co-workers. They demonstrate that the suppression of endogenous E2 synthesis by letrozole treatments for 4 days significantly decreases the density of spines, spine-synapses, spinophilin (spine marker) and synaptophysin (presynaptic marker) in CA1 of cultured slices [5]. Application of 100 nM E2 rescues the synaptophysin expression that was once decreased by letrozole treatments. However, when slice cultures are not treated with letrozole,
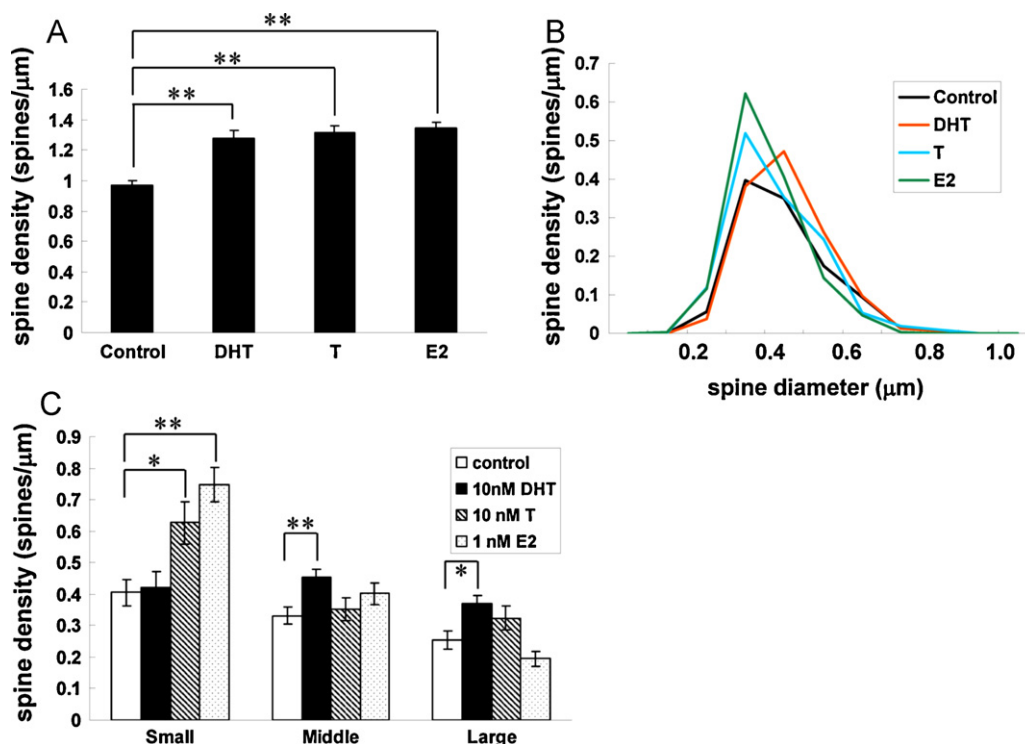
Fig. 5. Rapid modulation of spines by estrogen and androgen (adult male rat, 12 weeks). Spines were analyzed by Spiso-3D along the secondary dendrites in the stratum radiatum of CA1 pyramidal neurons. (A) Total spine density. A 2-h treatment in ACSF without hormone (Control), with 10 nM DHT, with 10 nM T and with 1 nM E2, 1.34 spines/μm. (B) Histogram of spine head diameters. After a 2-h treatment in ACSF without steroids (Control, black line), DHT (red line), T (blue line) and E2 (green line). (C) Density of three subtypes of spines with DHT, T and E2. From left to right, ACSF without steroids (open column), 10 nM DHT (filled column), 10 nM T (stripe column) and 1 nM E2 (dotted column). Vertical axis is the average number of spines per 1 μm. $*p < 0.05$, $**p < 0.01$ vs Control. (For interpretation of the references to color in this figure legend, the reader is referred to the web version of the article.)
Modified from Mukai et al. [38].

application of 100 nM E2 does not further increase the spine density, spine-synapses or spinophilin expression. These no E2 effects can be explained due to the presence of endogenous high level E2 in slices (3–10 nM) which can prevent exogenous E2 effects [52].

Compared with the case of estrogen, androgenic regulation on the formation and morphologic changes of dendritic spines has been poorly understood in the hippocampus. Leranth and co-workers report that T is important for maintenance of normal spine density in male rat hippocampus, because the 2-day application of T propionate or DHT retrieves the spine density in CA1 pyramidal neurons of gonadectomized rats in which the density is reduced without androgen supplement [53]. A part of the effects of T on dendritic spines in females, not in males, seems to be mediated by local conversion to estradiol [54]. The rapid enhancement (within 2 h) by T and DHT of spines also occurs in CA1 and CA3 [55].

2.3. Synaptic (extranuclear) receptors for estrogen and androgen (Fig. 6)

What is the receptor of 17β-E2 that mediates rapid actions (1–2 h) on synaptic plasticity in the hippocampus? Putative synaptic membrane estrogen receptors remain poorly defined. Many attempts have been made to identify membrane estrogen receptors. At the present stage, the most probable candidates for synaptic (extranuclear) estrogen receptors may be ERα and ERβ [18]. Although ERα and ERβ are classical nuclear receptors, they may work very differently at synapses, for example, driving kinases, metabotropic glutamate receptor (mGluR) or G-protein [16,18,37,57–59].

We identify the membrane estrogen receptor ERα localized in the spines of hippocampal pyramidal and granule neurons (from adult male rats) by means of immunoelectron microscopic analysis as well as Western blot analysis, using affinity-column purified anti-ERα antibody RC-19 (C-terminal antibody) [16,18]. Attention must be paid to the fact that non-purified ERα antisera often react significantly with unknown proteins (62 kDa protein in the brain, Western blot), resulting in incorrect staining which differs from the real ERα distribution. In hippocampal slices the expression of 62 kDa protein is nearly the same as that of ERα, however, the cerebellum has a significant expression of 62 kDa protein, although real ERα expression is very poor [16]. A post-embedding immunogold electron microscopic analysis demonstrates the synaptic localization of ERα in the glutamatergic neurons in CA1, CA3 and DG (Fig. 6). ERα is also localized in the nuclei. Western blot analysis demonstrates that ERα (67 kDa) and MAPK are tightly associated with postsynaptic density fractions (PSD) (Fig. 6). On the other hand, ERα is not expressed at dendritic raft which is rich in caveolin in adult male hippocampus [18]. Because the E2-induced modulation of LTD and spine density appears so rapidly in the time range of 1–2 h, the synaptic ERα observed at PSD or postsynaptic compartments probably plays an essential role in driving rapid signaling. Interestingly, a significant accumulation of ERα at PSD was observed by a 3 min stimulation with 30 μM NMDA used for the LTD induction, implying that ERα may be dynamically movable in spines or dendrites [18]. The specific binding of purified RC-19 antibody to real ERα (67 kDa) in the hippocampus is verified as the absence of reactivity of RC-19 with ERα knock-out mice hippocampus (Fig. 6) [16]. These analyses are essential in the hippocampus and other brain regions, as we found that non-purified MC-20 antisera, frequently used in investigations, often react with unknown 62 kDa proteins in
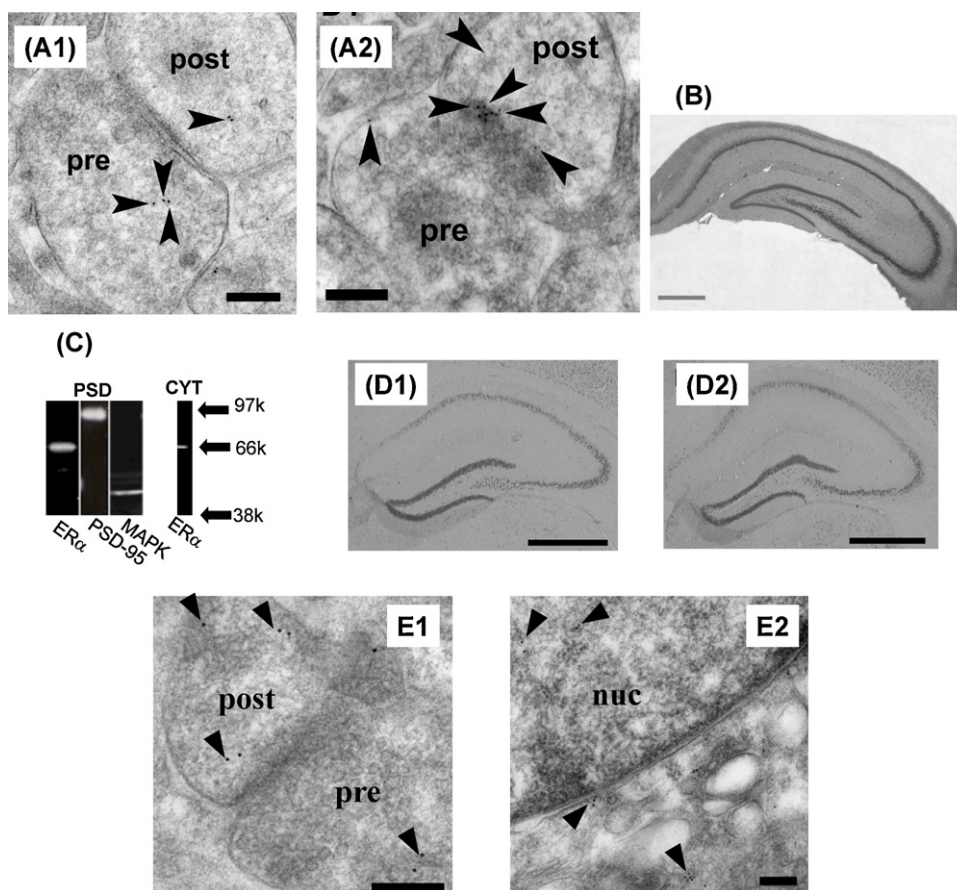
Fig. 6. Synaptic localization and neuronal expression of ERα and GR in adult male rat. (A) Immunoelectron microscopic analysis of the distribution of ERα within axospinous synapses, in the stratum radiatum of hippocampal CA1 neurons. (A1) Gold particles (arrowheads) are localized in the pre- and postsynaptic regions. (A2) In dendritic spines, gold particles are associated with PSD regions. Pre, presynaptic region; post, postsynaptic region. Scale bar: 200 nm. (B) Immunohistochemistry of ERα (with RC-19) showing expression of ERα in pyramidal neurons (CA1–CA3) as well as granule cells (DG). (C) Western blot of ERα in postsynaptic density (PSD) and cytoplasmic (CYT) fractions of the hippocampus. From left to middle, blot of PSD fraction with RC-19 IgG (ERα), PSD-95 IgG (PSD-95) and MAP kinase IgG (MAPK). Right, blot of CYT fraction with RC-19 (ERα). The applied protein amount was 3-fold greater for PSD fraction than for CYT fractions. (D) MC-20 antiserum binds to both ERαKO mice (D1) and wild mice (D2), indicating that MC-20 binds to an unknown protein different from ERα. Scale bar: 50 μm for (A1) and (B1). Several different batches of MC-20 are used. (E) Immunoelectron microscopic analysis of the GR localization within axospinous synapses, in the stratum radiatum of hippocampal CA1 neurons. (E1) Gold particles (arrow) are localized in the pre- and postsynaptic regions. (E2) Gold particles are also localized in the nuclei. Pre, presynaptic region; post, postsynaptic region. Scale bar: 200 nm.
Modified from Mukai et al. [16] and Ooishi et al. (2011).

several brain regions, and do not significantly react with true ERα (67 kDa) (Fig. 6) [16]. ERα antisera are often verified for their reactivity only in endocrine organs such as the ovary, in which ERα is highly expressed. Therefore, the staining of interneurons and absence of staining of primary neurons with non-purified antisera (such as MC-20 or AS409) probably do not show the true ERα distribution in the hippocampus (Fig. 6) [16,18]. Antisera should be purified before application to the hippocampus. ERα knock-out mice may be useful in investigating the participation of ERα in modulation of synaptic plasticity. However, thus far, no data is available for true ERα knock-out mice. Electrophysiological investigations are performed by using knock-down mice (not knock-out mice) by Moss and coworkers [43,60]. They report no essential contribution of ERα to the E2-induced rapid enhancement of the kainate currents of CA1 neurons. They reach this conclusion due to the observation of a very small difference in the E2 effect on the kainate currents between wild-type and ERα-Neo knock-down mice which have been constructed by the method of Neomycin insertion into exon 1 (the previously named exon 2) [61]. However, in Neomycin-inserted ERα-Neo knock-down mice, N-terminal-modified ERα (61 kDa) is expressed [61–63]. Because the N-terminal-modified ERα still binds E2 and drives genomic processes [61–63], the

participation of ERα in the electrophysiological properties of the CA1 cannot be excluded from their investigations. Therefore, it is necessary to investigate true ERα knock-out mice in which, for example the whole exon 2 of the mouse ERα gene is deleted [64].

As an another example, Mermelstein and co-workers have indicated that membrane associated ERα interacts with mGluR via caveolin coupled with G protein in female primary cultured hippocampal neurons [57–59]. E2 very rapidly (in the time scale of 5 min) phosphorylates CREB by MAP kinase via Gq, and these events are prevented by mGluR1a inhibitor or ICI. Interestingly, these events occur particularly in female neurons and not in male neurons [57].

We still have paradoxical results concerning membrane ERα and ERβ in electrophysiological properties. Since ICI does not suppress E2-induced rapid modulation of electrophysiological properties, such as LTD, LTP, and kainate-induced currents, many scientists consider that classical estrogen receptors are not involved in these modulations [43]. However, these results do not eliminate the possibility that ERα and ERβ could modulate these synaptic transmissions, because ICI has been indicated to display its effect by inhibiting the dimerization of ERα and ERβ. If dimerization

processes are not involved in the rapid modulation of electrophysiological phenomena, then ICI cannot block these phenomena. On the other hand, the rapid enhancement of spinogenesis via ERα is significantly blocked by ICI [16], therefore, dimerization processes of synaptic ERα occur in spinogenesis. Selective ERα or ERβ antagonists, such as MPP or PHTPP, may be useful to identify E2 receptors responsible for modulation of synaptic transmission (LTP, LTD).

Accumulated results support that ERβ acts as a membrane receptor or synaptic receptor. ERβ associates with membranes in genetically expressed CHO cells and MCF-7 cells [65,66]. ERβ rapidly attenuates LTD-induction [16] and rescues CORT-induced suppression of LTP. ERβ rapidly prevents phosphorylation of CREB through mGluR2 and Gi via L-type calcium channel in primary cultured hippocampal neurons [57]. Several investigations of immunostaining of ERβ suggest the extranuclear expression of ERβ including dendritic appearance in the hippocampal principal neurons [68]. The subcellular immunostaining patterns of these reports might reflect the relatively minor expression of ERβ and the major expression of unknown proteins, due to multiple reactivity of non-purified ERβ antisera to several unknown proteins observed in the Western blot analysis of hippocampal tissues. The purity of commercially available ERβ antisera is worse than that of ERα antisera as judged from our Western blot analysis.

Transmembrane G-protein coupled estrogen receptor GPR30 is an another candidate of membrane estrogen receptor observed in SKBR3 breast cancer cells that lack ERα and ERβ [69], as well as in COS7 after genetic expression of GPR30 fused with green fluorescent protein [70]. The expression of GPR30 is also observed in hippocampal neurons [33,71]. Synaptic expression of GPR30, however, has yet to be demonstrated, and further investigations are necessary to reveal its contribution to the rapid E2 modulation of synaptic plasticity. For these investigations ICI could be used as GPR30 agonist.

3. Synthesis of sex steroids in the hippocampus

3.1. Pathway of synthesis (Fig. 7)

Sex steroids had been thought to reach the brain exclusively via blood circulation after crossing the blood–brain barrier [72]. However, recent studies using immunohistochemical staining and Western immunoblot analysis reveal a significant localization of steroidogenic proteins such as cytochromes P450scc, P450 (17α), P450arom and StAR in pyramidal neurons in CA1–CA3, as well as in granule cells in DG, of adult hippocampus (12 week) (Fig. 7) [1–4,18,73], and also developmental hippocampus [5,74–76]. Interestingly, synaptic localization of P450(17α), P450arom was demonstrated by immunogold electron microscopic analysis, implying synaptocrine mechanisms [4,37,76,78]. The hippocampal expression of mRNAs for steroidogenic enzymes is also demonstrated using RT-PCR and/or in situ hybridization for P450scc [79,80], StAR [81,82], 3β-hydroxysteroid dehydrogenase (3β-HSD) [81,83], P450(17α) [4], P450arom (CYP19) [4,84,85], 17β-hydroxysteroid dehydrogenase (17β-HSD) type 1–4 [4,86], and 5α-reductase [78,87]. These results imply that hippocampal pyramidal neurons and granule neurons are equipped with complete steroidogenic systems which catalyze the conversion of cholesterol to pregnenolone (PREG), dehydroepiandrosterone (DHEA), T and E2.

3.2. Developmental and age-related change of steroidogenic enzymes or sex-steroid receptors

Exhaustive analysis of age-dependent expression for these steroidogenic enzymes indicates moderate decrease of their expressions [33]. Comparison of relative expression levels of enzymes is shown in Table 1. Contrary to the widely held belief,
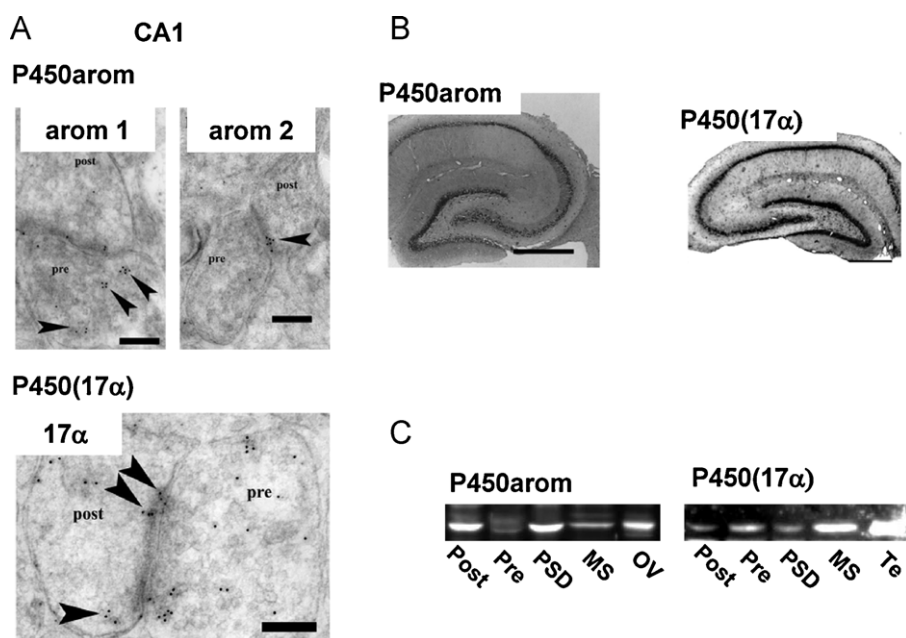

Fig. 7. Sex-hormone synthase cytochrome P450; synaptic localization and neuronal expression (adult male rat). (A) Immunoelectron microscopic analysis of the distribution of P450arom and P450(17α) within synapses, in the hippocampal CA1 (arom 1, 2 and 17α). Gold particles (indicated by arrow heads) are observed to be localized in the presynaptic region (pre), and the postsynaptic region (post) of pyramidal neurons in CA1 and CA3, and granule neurons in DG. In the presynaptic region (pre), gold particles are associated with small synaptic vesicles. In spines (post), gold particles are found within the spine heads. Scale bar: 200 nm for arom 1, 2 and 17α. (B) Immunohistochemical staining of P450arom and P450(17α) in the coronal section of adult male rat hippocampus. Scale bar: 800 μm. (C) Western immunoblot analysis of P450arom and P450(17α) in subcellular fractions of adult male rat hippocampus. From left to right, postsynaptic membrane-rich fraction (post), presynaptic membrane-rich fraction (pre), postsynaptic density fraction (PSD), microsomes (MS) and ovary (OV) for P450arom, and post, pre, PSD, MS and testis (Te) for P450(17α). The amount of protein applied to the gels was 20 μg for each hippocampal fraction, and 1 μg for ovary or testis.
Modified from Hojo et al. [4] and Mukai et al. [33].

Table 1
Age-dependent change of mRNA expression of steroidogenic enzymes and receptors.

	Relative expression level at PD1 (%)	Relative expression level at postnatal 12 week (PW12) (%)
3β-HSD I	100	100 = 56% of PD1 level
Cyp11a1	800	900
Hsd17b1	24,000	22,800
Hsd17b3	4800	12,600
Cyp19a1	460	510
Esr1	16,000	22,500
Esr2	1600	2100
Srd5a1	820,000	1,350,000
Srd5a2	12,000	8900
Ar	38,000	220,000
Sf-1	153	65

the expression level of steroidogenic enzymes or sex-steroid receptors do not decrease considerably depending on development from PD1 (postnatal day 1) to PW12 (postnatal 12 week, young adult), but steroidogenic enzymes or sex-steroid receptors still expressed 50–70% level of PD1 at PW12 (Fig. 8). Almost no decrease was even observed for 5α-reductase (type 1, Sd5a1). Exceptionally, a large decrease of P450scc occurs at PW4–PW12 down to approx. 7% of PD1, although a high level of PREG (approx.37 nM) is observed in the hippocampus [1]. Since circulating PREG is only 2 nM [1], how this high level of PREG pool can be maintained in the hippocampus?

Estrogen receptors ERα/ERβ also gradually decrease to approx. 70% of PD1 at PW12. In contrast, androgen receptor AR gradually increases to approx 330% of PD1 at PW12. These results suggest that effects of estrogen may be stronger between PD1 and PD10

than those of androgen which may become stronger in young adult days.

Interestingly, steroidogenic factor 1 (Sf-1/AD4BP) is moderately expressed in the hippocampus [33,85]. The expression level of Sf-1 is even higher (approx. 150% at PD1) than that of 3β-HSD I, and the level decreased moderately to 12 weeks. Therefore, the regulation of steroidogenic enzymes may be similar to that in peripheral organs such as testis or ovary [88].

Although the relative expression levels of mRNAs for the hippocampal sex-steroidogenic enzymes are in the order of 1/200–1/1000, as compared with their levels in gonads, these levels are not too low for them to produce sufficient amount of hippocampal sex steroids. They need to produce sex steroids that fill only a small hippocampal volume (approx. 0.14 mL at 12 weeks; approx. 1/200 of the blood volume of ~25 mL), whereas gonadal steroids need to fill the whole blood volume that is nearly 200-fold of the hippocampal volume. In fact, we observed that hippocampal levels of E2 and T (approx. 8 and 17 nM, respectively) were even higher than circulating levels (approx. 0.01 and 15 nM, respectively).

The neuronal synthesis of DHEA, T and E2 in adult mammals is demonstrated for the first time by Kawato and co-workers in the adult (12 week) hippocampal slices by means of careful HPLC analysis [1,2,4]. The significant conversion from [³H]-PREG to ³H-DHEA, from ³H-DHEA to ³H-androstenediol, to ³H-T and to ³H-E2 is observed after incubation with the slices for 5 h [4]. The rate of production for ³H-E2 from ³H-T is very slow, and the production rate of ³H-DHT from ³H-T is much more rapid than that of E2. These activities are abolished by the application of specific inhibitors of cytochrome P450s. Surprisingly, ³H-E2 is extremely stable and is not significantly converted to other steroid metabolites such as estrone. On the other hand, DHT is rapidly converted
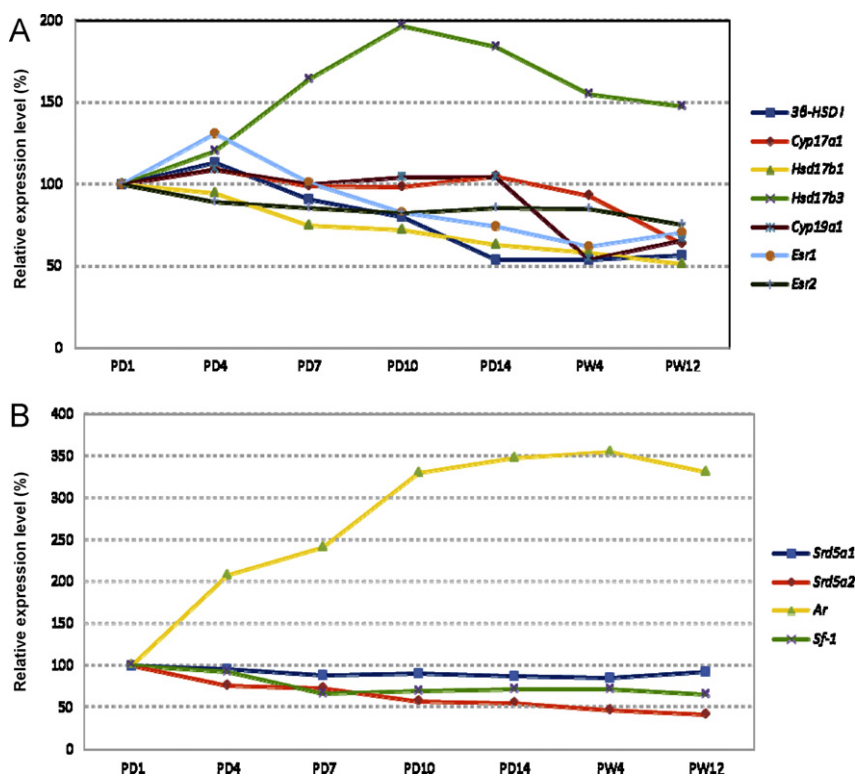
Fig. 8. Developmental age-related mRNA expression of steroidogenic enzymes and receptors in the hippocampus. (A) The age-related temporal changes in the mRNA expression of estrogen-synthesis enzymes as well as estrogen receptors. Relative expression levels of mRNAs is indicated as the ratio to that at PD1 (PD1 was set to be 100% for each gene). 3β-HSDI, Cyp17a1[P450(17α)], Hsd17b1,3[17β-HSD1,3], Cyp19a1[P450arom], Ers1[ERα] and Ers2[ERβ]. (B) The age-related temporal changes in the mRNA expression androgen-synthesis enzymes as well as androgen receptors. Sd5a1,2[5α-reductase type1,2], Ar[Ar] and Sf-1[SF-1]. Relative expression levels of mRNAs is indicated as the ratio to that at PD1 (PD1 was set to be 100% for each gene). The level of sf-1 is higher (153% at PD1) than that of 3β-HSD I.
Modified from Kimoto et al. [88].

to 3α,5α-androstanediol. To demonstrate the rapid net production of neurosteroids upon synaptic stimulation, the NMDA-induced production of PREG and E2 is investigated in hippocampal slices [1,2,4]. Upon stimulation with NMDA for 30 min, the hippocampal levels of PREG and E2 increase to approx. 2-fold that of the basal levels. This implies that the NMDA-induced Ca^{2+} influx drives the net production of PREG and E2. E2 synthesis is also demonstrated in cultured hippocampal slices from neonatal rats in the absence and presence of letrozole, an inhibitor of P450arom. After a 4 day treatment with letrozole, the amount of E2 released into the medium is significantly decreased [5].

3.3. Concentration of estrogen and androgen (Fig. 9)

Why do we need E2 concentrations higher than 1 nM in order to obtain significant effects of E2 in brain slices or neurons? Does this suggest that the endogenous concentration of E2 in the brain is higher than 1 nM ? Such a high level of E2 cannot be supplied from circulation, because the maximal circulating E2 level achieved in cycling female rats is 0.1 nM at proestrus. To answer these questions, an accurate determination of the concentration of E2 and other steroids is necessary for an understanding/explanation of its modulatory action on synaptic plasticity including LTP, LTD or spinogenesis.

In most cases, scientists did not know or cold not measure the endogenous E2 level in brain slices or cultured neurons. From our reliable determination, the hippocampal E2 concentration is much higher than that in circulation, although the absolute amount E2 is very small due to the small volume of hippocampal tissues. In addition, the concentration of E2 in ACSF-treated slices is not invariant and is often very different from that in freshly isolated hippocampal tissues. Because of technical problems including poor purification procedures of steroids from fatty brain tissues, the accurate determination of the E2 concentration in whole hippocampal tissues, slices or cultured neurons had been difficult. By combination of steroid purification with solid phase C18 column and radioimmunoassay (RIA), the concentration of E2 was determined to be approx. 0.6 nM (basal) and 1.3 nM after the NMDA-stimulation, respectively, in the adult male rat hippocampus [4]. RIA is a very sensitive method for steroid detection, but has uncertainty regarding specificity and accuracy due to problems of antisera used.

For a direct determination of steroids, mass-spectrometric assay is much better than RIA. As an impressive example, the absence of PREG-sulfate in the rat/mouse brain was indicated by mass-spectrometric assay [89–91]. Earlier studies had assumed the presence of PREG-sulfate. Therefore after solvolysis of water-soluble fractions to convert virtual PREG-sulfate to PREG, scientists detected PREG by RIA [1,90,92–94]. Water-soluble fractions might contain water soluble micelles containing some PREG derivatives. Because PREG-sulfate had been extensively studies as a representative neuromodulator, these results merit careful consideration of neurosteroid research [72,95,96].

What about the concentration of 17β-E2 in the brain? The presence of 17β-E2, DHT and estrone (E1) had not yet been observed even by mass-spectrometric assay including gas chromatography with mass-spectrometry (GC–MS/MS), liquid chromatography with mass-spectrometry (LC–MS) and liquid chromatography with tandem-mass-spectrometry (LC–MS/MS), although DHEA and T have been observed in the whole brain extracts [89,90,94,97,98].

We therefore substantially improved the determination methodology using liquid chromatography–tandem-mass spectrometry (LC–MS/MS) in combination with picolinoyl-derivatization (for induced ionization) of pre-purified E2/T/DHT/E1 fractions obtained from purification by normal phase HPLC [78,99]. E2 was further derivatized with pentafluorobenzyl in order to elevate evaporation probability. We achieved the good limits of quantification which are 0.3 pg (17β-E2) and 1 pg (T, DHT, E1) per 0.1 g of hippocampal tissue or 1 mL of plasma, respectively.

Pre-purification of E2/T/DHT/E1 fractions via normal phase HPLC is necessary to remove contaminating fats, lipids and mixed steroids, since reverse phase LC included in LC–MS/MS is not suitable for this kind of purification of non-charged steroids. By improved LC–MS/MS analysis, average basal level of E2 is determined to be approx. 8 nM in the hippocampus of male rats (Fig. 9) [18].

From LC–MS/MS analysis of male hippocampal tissues, the average level of E2, T and DHT is approx. 8 nM, 17 nM and 7 nM, respectively (Fig. 9). Surprisingly, the E2 level is not decreased by castration to deplete circulating T which is a precursor for E2 synthesis (Fig. 9) [78]. On the other hand, castration decreases hippocampal T to 3 nM which is hippocampus-synthesized T. Hippocampal E2 may be preferentially synthesized from hippocampal T, rather than from circulating T which is preferentially converted to DHT, since castration decreases hippocampal DHT considerably to 0.2 nM (Fig. 9-1).

It should be noted that the level of E2 in adult hippocampus (reported from other labs) does not fall in the same range as that of our observation that demonstrates nanomolar level of E2. For example, only approx. 35 pM E2 (10 pg/g wet weight) was observed by RIA in postnatal 60 days of male rat hippocampus, which showed age-related decrease from 0.5 nM (140 pg/g wet weight) at PD0 [100].

In the case of cultured slices or cultured neuron/glia, the endogenous E2 level may be approx. 5 nM (50 fmol/mg protein) in slices determined via RIA or mass-spectrometric assay [52] or 0.03–0.1 nM in the outer medium (released E2) [5,75,101]. Therefore, the concentration of exogenously applied E2 should be higher than the endogenous E2 level, in order to show E2 effects.

Attention must be paid to 'acute' hippocampal slices which are often used for electrophysiological or spinogenesis experiments. During preparation of 'acute' slices in steroid-free ACSF for 1–2 h (recovery incubation), endogenous steroids are depleted, resulting in E2 concentration less than 0.5 nM (Fig. 9-2). Therefore, supplementation of E2 (1–10 nM) to 'acute' slices shows clear effects [6,7,9,16,22,43]. Probably E2 (1–10 nM) cannot induce any effect in cultured slices which keep endogenous 5–8 nM E2 level. In this sense, these 'acute' slice experiments may represent an *in vitro* model of *in vivo* estrogen replacement therapy in which circulating estrogen-depleted ovariectomized female rats (hippocampal E2 of 0.2 nM) are injected with E2 at 10–50 μg/kg rat weight.

One of the functional differences between E2 produced from circulating T and E2 produced from hippocampus-derived T may be the regulation of synthesis. The brain is permeated with circulating T (male), or E2 (female), the levels of which change slowly depending on the circadian rhythm. On the other hand, the endogenous synthesis of E2 (for both male and female) may be transient events depending on neural excitation such as an LTP or LTD event, because the E2 level is significantly elevated upon Ca^{2+} influx by NMDA stimulation [4]. Synaptic localization of steroidogenic enzymes support this kind of synaptocrinology events that are triggered by activation of StAR upon Ca^{2+} influx through NMDA receptors.

Another functional difference between hippocampal sex-steroids and circulating sex-steroids might be the fractions of free/active steroids. Nearly all hippocampal sex-steroids could be free and active inside of neurons, because carriers of sex-steroid [SHBG (sex-steroid binding globulin) and serum albumin] are absent within neurons. In circulation, nearly 95% of estrogen and androgen may be inactive, because they bind to SHBG or serum albumin in order to circulate through blood vessels. Therefore, hippocampal sex-steroids are much higher in concentration and in modulation activity than circulating sex-steroids.
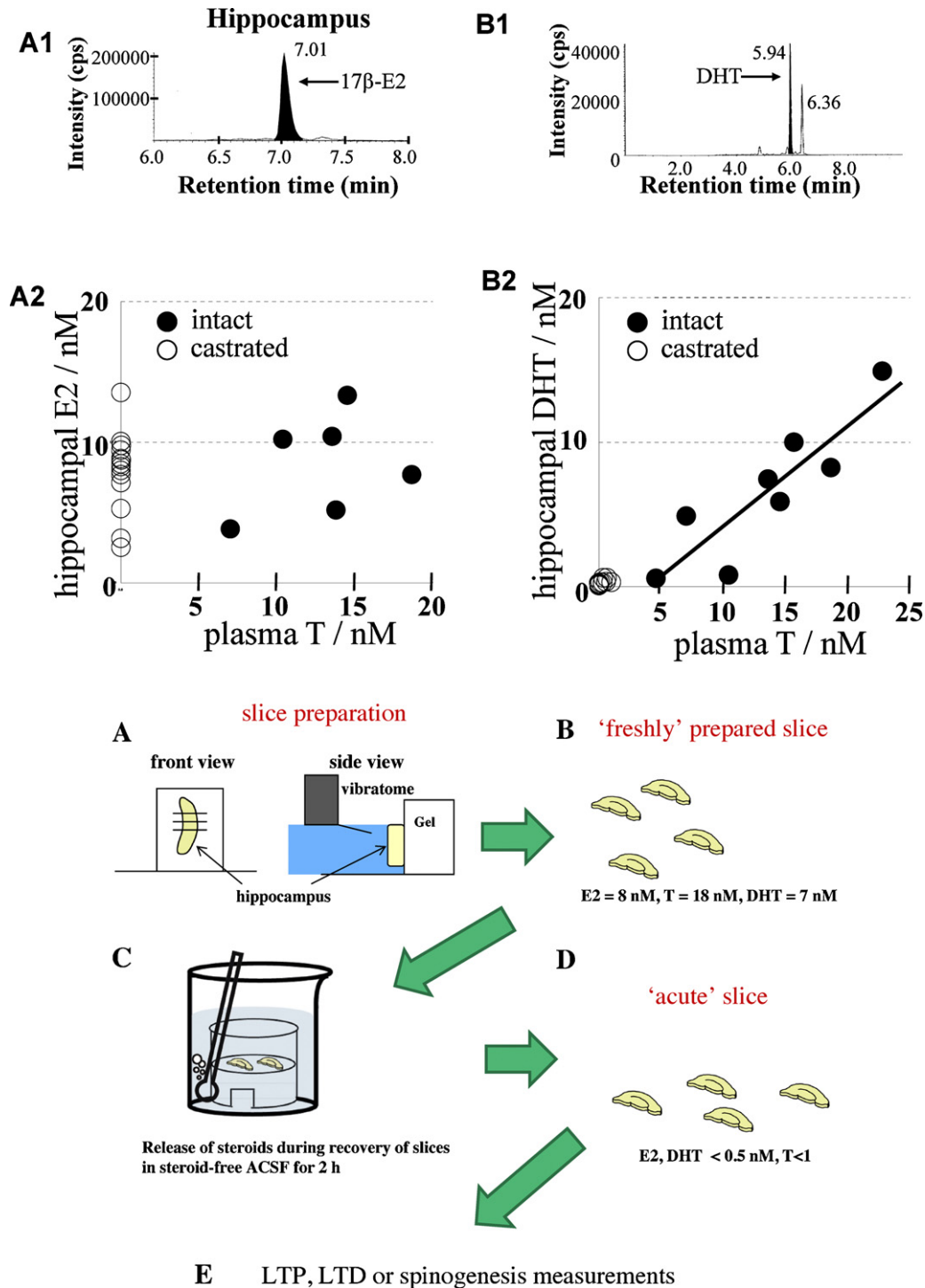
Fig. 9. (1) Mass-spectrometric determination of sex-steroids (adult hippocampus). LC–MS/MS chromatograms and steroid derivatives of (A1) 17β-E2 and (B1) DHT. Shaded portions indicate the intensity of the fragmented ions of 17β-E2-pentafluorobenzoxy-picolinoyl ($m/z = 339$, A1) and DHT-picolinoyl ($m/z = 203$, B1), respectively. The horizontal axis indicates the retention time of the fragmented ions. (A2) No effect of castration on hippocampal E2 level as well as no correlation between plasma T and hippocampal E2. (B2) Considerable effect of castration on hippocampal DHT level as well as a good correlation between plasma T and hippocampal DHT. These data suggest that hippocampal E2 is primarily produced from hippocampus-synthesized T, and that hippocampal DHT is primarily produced from circulating T by 5α-reductase in the hippocampus. Note that plasma DHT is very low at approx. 0.6 nM even in intact rats. Closed circle, intact rats; open circle, castrated rats. [Modified from Hojo et al. [78].] (2) Schematic illustration of significant depletion in sex-steroids by preparation of 'acute' slices, used for measurements of LTP, LTD and spinogenesis.

4. Difference between classical slow genomic modulation and rapid synaptic modulation by estrogen

Not only slow (gene transcriptional) but also rapid (kinase driving) estrogen signaling occurs independently in the brain (Fig. 10).

4.1. Slow action via genomic pathway

Classical genomic effects have been studied extensively in the past few decades, focusing mainly on restorative effects on brain function by supplemented estrogen in ovariectomized female rats. In classical slow genomic pathway, gonadal E2 → reaches neurons
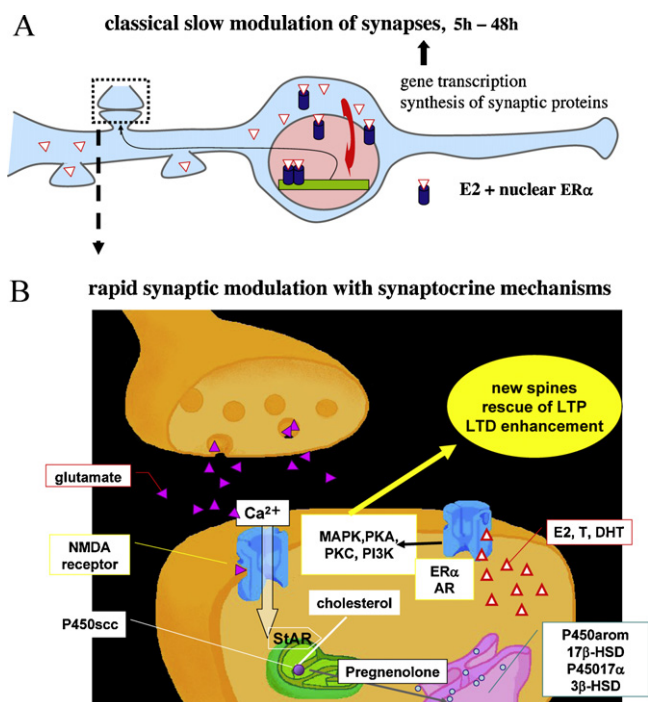
Fig. 10. Schematic illustration. (A) Slow modulation of synaptic plasticity via gene transcription and synthesis of synaptic proteins in neurons. The site of the delayed action of E2 is ERα/ERβ in cytoplasm and nuclei. New synaptic connections are formed by synthesized synaptic proteins or neurotrophic factors. The neuronal synthesis (intracrine mechanism) of sex-steroids produces much higher level of E2 than E2 from circulation. StAR and P450scc are present in the mitochondria, and P450(17α), 3β-HSD, 17β-HSD and P450arom are localized in the endoplasmic reticulum. (B) Rapid modulation of the synaptic plasticity via synaptic ERα. Synaptic ERβ may also function. Kinases or CREB may also induce gene transcription. Synaptic synthesis (synaptocrinology mechanism) of sex hormones is driven by StAR activation by Ca²⁺-influx through NMDA receptors [1], followed by catalysis via P450scc, P450(17α), 17β-HSD, 3β-HSD and P450arom. Ca²⁺-influx may drive activation of P450arom via (phosphatase-dependent) dephosphorylation [111]. The membranes in the synaptic compartment. Only NMDA type glutamate receptor is illustrated, while AMPA type glutamate receptor is omitted for clarity.

via the circulation → cytoplasmic ERα or ERβ → nucleus → gene transcription → new synaptic proteins (NMDA-R NR1 subunit, brain-derived neurotrophic factor (BDNF), etc.) → synaptogenesis, enhancement of LTP and neuroprotection. Because the activation of both the transcriptional and translational machinery of the cell is necessary to invoke classical steroid actions, a time-lag of several hours to days must be present between the beginning of the steroid action and its physiological consequences.

The chronic genomic effects of E2 on synaptic plasticity have been extensively investigated. For example, the dendritic spine density in CA1 pyramidal neurons is sensitive to both naturally occurring estrogen fluctuations in rats [10], and experimentally induced estrogen depletion and replacement [45]. Estrogens mediate these morphological changes in correlation with NMDA receptors. E2 increases the binding of NMDA or glutamate to NMDA receptors, as well as the NR1 level in CA1 dendrites [49,50,102]. Moreover, the estrogen-induced increase in dendritic spine density is blocked by NMDA receptor antagonists [11,51,103], and the electrophysiological properties of NMDA receptor-mediated transmission are altered by estrogen [7,8,32].

4.2. Gene transcription as a downstream event of rapid synaptic action

Rapid synaptic actions of E2 are not limited to those within synapses but also may include the triggering of gene transcription

in nuclei. Many kinases (MAPK, PKA, PI3K, PKC, etc.) are activated in the rapid synaptic actions of E2 [17,35,37,104–106]. These kinases (or phosphorylated transcription factors) may also travel to nuclei, resulting in gene transcription and production of synaptic proteins. For example, PKA → phosphorylation of CREB → gene transcription → new synaptic protein → new synapses [107]; MAPK → gene transcription → new synaptic protein → new synapses → protection of neuron from damage [107]; PI3K → Akt kinase → suppression of GSK-3β → suppression of hyperphosphorylation of tau → inhibition of disassembling of microtubles → protection from Alzheimer's disease [108,109]; PI3K → Akt kinase → suppression of apoptosis signal from mitochondria → protection of neuron from damage; PKC → NFκB → gene transcription → new protein → new synapses [110].

5. Model explanation of modulation of synaptic plasticity by sex steroids in relation to synaptocrine and intracrine mechanisms (Fig. 10)

Rapid modulation is triggered by E2 binding to synaptic ERα, resulting in activation of many kinases (MAPK, PKA, PKC, PI3K or even phosphatases), followed by modulation of NMDA receptors (NMDA type glutamatergic receptors) or AMPA receptors (AMPA type glutamatergic receptors). E2-induced phosphorylation of NR2B subunit by MAPK activation occurs [24]. E2-induced phosphorylation of AMPA receptors by these kinases is not well examined. For spine formation, MAPK induced phosphorylation of cortactin may drive new spine formation via polymerization of actin fibers.

The synaptic synthesis of sex steroids (synaptocrine mechanism) proceeds in the following manner. First, glutamate release from the presynapse induces a Ca²⁺ influx through the NMDA receptors. The Ca²⁺ influx drives StAR to transport cholesterol into the mitochondria, where P450scc converts cholesterol to PREG. Multiple pathways exist in downstream including (1) PREG → DHEA → androstenediol → T, (2) PREG → progesterone (PROG) → androstenedione → T, (3) T → E2, or (4) T → DHT, These synthesis reactions are performed in spines, in addition to the endoplasmic reticulum in the cell body by P450(17α), 17β-HSD, 3β-HSD, P450arom and 5α-reductase.

Note that sex steroids are synthesized also in mitochondria and the endoplasmic reticulum in the cell bodies of neurons (intracrine mechanisms). The genomic pathway via nuclear ERα/ERβ receptors also functions in genomic E2 effects, including synthesis of synaptic proteins (intracrine mechanisms). Because the levels of E2, T and DHT are much lower in the circulation [18,78], hippocampus-synthesized sex-steroids may play a central role in the modulation of synaptic plasticity or memory processes.

An immunoelectron microscopic analysis using a postembedding immunogold method is very useful in determining the intraneuronal localization of P450 or ERα in the hippocampal neurons. Surprisingly, we observed that P450(17α), P450arom and ERα are localized not only in the endoplasmic reticulum but also in the postsynaptic region as well as the presynaptic region of pyramidal neurons in the CA1 and CA3 regions and granule neurons in DG (Figs. 6 and 7). These results imply the 'synaptic' synthesis of estrogen and androgen, in addition to classical microsomal synthesis of sex steroids. Synaptic E2 level is therefore locally high enough to drive synaptic ERα.

References

[1] T. Kimoto, T. Tsurugizawa, Y. Ohta, J. Makino, H. Tamura, Y. Hojo, N. Takata, S. Kawato, Endocrinology 142 (2001) 3578–3589.
[2] S. Kawato, Y. Hojo, T. Kimoto, Methods Enzymol. 357 (2002) 241–249.

[3] S. Kawato, M. Yamada, T. Kimoto, Adv. Biophys. 37 (2003) 1–48.
[4] Y. Hojo, T.A. Hattori, T. Enami, A. Furukawa, K. Suzuki, H.T. Ishii, H. Mukai, J.H. Morrison, W.G. Janssen, S. Kominami, N. Harada, T. Kimoto, S. Kawato, Proc. Natl. Acad. Sci. U.S.A. 101 (2004) 865–870.
[5] O. Kretz, L. Fester, U. Wehrenberg, L. Zhou, S. Brauckmann, S. Zhao, J. Prange-Kiel, T. Naumann, H. Jarry, M. Frotscher, G.M. Rune, J. Neurosci. 24 (2004) 5913–5921.
[6] R. Bi, G. Broutman, M.R. Foy, R.F. Thompson, M. Baudry, Proc. Natl. Acad. Sci. U.S.A. 97 (2000) 3602–3607.
[7] M.R. Foy, J. Xu, X. Xie, R.D. Brinton, R.F. Thompson, T.W. Berger, J. Neurophysiol. 81 (1999) 925–929.
[8] L.D. Pozzo-Miller, T. Inoue, D.D. Murphy, J. Neurophysiol. 81 (1999) 1404–1411.
[9] K. Shibuya, N. Takata, Y. Hojo, A. Furukawa, N. Yasumatsu, T. Kimoto, T. Enami, K. Suzuki, N. Tanabe, H. Ishii, H. Mukai, T. Takahashi, T.A. Hattori, S. Kawato, Biochim. Biophys. Acta 1619 (2003) 301–316.
[10] C.S. Woolley, Horm. Behav. 34 (1998) 140–148.
[11] C.S. Woolley, B.S. McEwen, J. Neurosci. 14 (1994) 7680–7687.
[12] C.C. Smith, L.L. McMahon, J. Neurosci. 26 (2006) 8517–8522.
[13] M.A. Snyder, B.M. Cooke, C.S. Woolley, Hippocampus 21 (2011) 398–408.
[14] H. Mukai, N. Takata, H.T. Ishii, N. Tanabe, Y. Hojo, A. Furukawa, T. Kimoto, S. Kawato, Neuroscience 138 (2006) 757–764.
[15] T.J. Teyler, R.M. Vardaris, D. Lewis, A.B. Rawitch, Science 209 (1980) 1017–1018.
[16] H. Mukai, T. Tsurugizawa, G. Murakami, S. Kominami, H. Ishii, M. Ogiue-Ikeda, N. Takata, N. Tanabe, A. Furukawa, Y. Hojo, Y. Ooishi, J.H. Morrison, W.G. Janssen, J.A. Rose, P. Chambon, S. Kato, S. Izumi, T. Yamazaki, T. Kimoto, S. Kawato, J. Neurochem. 100 (2007) 950–967.
[17] T. Tsurugizawa, H. Mukai, N. Tanabe, G. Murakami, Y. Hojo, S. Kominami, K. Mitsuhashi, Y. Komatsuzaki, J.H. Morrison, W.G. Janssen, T. Kimoto, S. Kawato, Biochem. Biophys. Res. Commun. 337 (2005) 1345–1352.
[18] Y. Hojo, G. Murakami, H. Mukai, S. Higo, Y. Hatanaka, M. Ogiue-Ikeda, H. Ishii, T. Kimoto, S. Kawato, Mol. Cell. Endocrinol. 290 (2008) 31–43.
[19] E.A. Kramar, L.Y. Chen, N.J. Brandon, C.S. Rex, F. Liu, C.M. Gall, G. Lynch, J. Neurosci. 29 (2009) 12982–12993.
[20] M. Ogiue-Ikeda, N. Tanabe, H. Mukai, Y. Hojo, G. Murakami, T. Tsurugizawa, N. Takata, T. Kimoto, S. Kawato, Brain Res. Rev. 57 (2008) 363–375.
[21] S. Kawato, Environ. Sci. 11 (2004) 1–14.
[22] K. Ito, K.L. Skinkle, T.P. Hicks, J. Physiol. 515 (Pt. 1) (1999) 209–220.
[23] R.M. Vouimba, M.R. Foy, J.G. Foy, R.F. Thompson, Brain Res. Bull. 53 (2000) 783–787.
[24] Y. Ooishi, H. Mukai, Y. Hojo, G. Murakami, Y. Hasegawa, T. Shindo, J.H. Morrison, T. Kimoto, S. Kawato, Cereb. Cortex (2011), in press, Web online.
[25] S. Higo, Y. Hojo, H. Ishii, Y. Komatsuzaki, Y. Ooishi, G. Murakami, H. Mukai, T. Yamazaki, D. Nakahara, T. Kimoto, S. Kawato, PLoS ONE 6 (7) (2011) e21631.
[26] M. Migaud, P. Charlesworth, M. Dempster, L.C. Webster, A.M. Watabe, M. Makhinson, Y. He, M.F. Ramsay, R.G. Morris, J.H. Morrison, T.J. O'Dell, S.G. Grant, Nature 396 (1998) 433–439.
[27] H.K. Lee, K. Kameyama, R.L. Huganir, M.F. Bear, Neuron 21 (1998) 1151–1162.
[28] J. Lisman, Proc. Natl. Acad. Sci. U.S.A. 86 (1989) 9574–9578.
[29] S.N. Yang, Y.G. Tang, R.S. Zucker, J. Neurophysiol. 81 (1999) 781–787.
[30] H. Mukai, T. Tsurugizawa, M. Ogiue-Ikeda, G. Murakami, Y. Hojo, H. Ishii, T. Kimoto, S. Kawato, Neuroendocrinology 84 (2006) 255–263.
[31] C.C. Smith, L.L. McMahon, J. Neurosci. 25 (2005) 7780–7791.
[32] D.A. Cordoba Montoya, H.F. Carrer, Brain Res. 778 (1997) 430–438.
[33] H. Mukai, T. Kimoto, Y. Hojo, S. Kawato, G. Murakami, S. Higo, Y. Hatanaka, M. Ogiue-Ikeda, Biochim. Biophys. Acta 1800 (2010) 1030–1044.
[34] Y. Komatsuzaki, G. Murakami, T. Tsurugizawa, H. Mukai, N. Tanabe, K. Mitsuhashi, M. Kawata, T. Kimoto, Y. Ooishi, S. Kawato, Biochem. Biophys. Res. Commun. 335 (2005) 1002–1007.
[35] G. Murakami, T. Tsurugizawa, Y. Hatanaka, Y. Komatsuzaki, N. Tanabe, H. Mukai, Y. Hojo, S. Kominami, T. Yamazaki, T. Kimoto, S. Kawato, Biochem. Biophys. Res. Commun. 351 (2006) 553–558.
[36] W.R. Harrington, S. Sheng, D.H. Barnett, L.N. Petz, J.A. Katzenellenbogen, B.S. Katzenellenbogen, Mol. Cell. Endocrinol. 206 (2003) 13–22.
[37] H. Ishii, T. Tsurugizawa, M. Ogiue-Ikeda, M. Asashima, H. Mukai, G. Murakami, Y. Hojo, T. Kimoto, S. Kawato, Neuroscientist 13 (2007) 323–334.
[38] H. Mukai, Y. Hatanaka, K. Mitsuhashi, Y. Hojo, Y. Komatsuzaki, R. Sato, G. Murakami, T. Kimoto, S. Kawato, Cereb. Cortex 21 (2011) 2704–2711.
[39] S.L. Wearne, A. Rodriguez, D.B. Ehlenberger, A.B. Rocher, S.C. Henderson, P.R. Hof, Neuroscience 136 (2005) 661–680.
[40] A. Rodriguez, D.B. Ehlenberger, D.L. Dickstein, P.R. Hof, S.L. Wearne, PLoS ONE 3 (2008) e1997.
[41] Y. Shinohara, H. Hirase, M. Watanabe, M. Itakura, M. Takahashi, R. Shigemoto, Proc. Natl. Acad. Sci. U.S.A. 105 (2008) 19498–19503.
[42] C.D. Kopec, E. Real, H.W. Kessels, R. Malinow, J. Neurosci. 27 (2007) 13706–13718.
[43] Q. Gu, R.L. Moss, J. Neurosci. 16 (1996) 3620–3629.
[44] N.J. MacLusky, V.N. Luine, T. Hajszan, C. Leranth, Endocrinology 146 (2005) 287–293.
[45] E. Gould, C.S. Woolley, M. Frankfurt, B.S. McEwen, J. Neurosci. 10 (1990) 1286–1291.
[46] C.S. Woolley, E. Gould, B.S. McEwen, Brain Res. 531 (1990) 225–231.
[47] C.S. Woolley, B.S. McEwen, J. Neurosci. 12 (1992) 2549–2554.
[48] C. Leranth, M. Shanabrough, T.L. Horvath, Neuroscience 101 (2000) 349–356.
[49] N.G. Weiland, Endocrinology 131 (1992) 662–668.
[50] A.H. Gazzaley, N.G. Weiland, B.S. McEwen, J.H. Morrison, J. Neurosci. 16 (1996) 6830–6838.
[51] D.D. Murphy, M. Segal, J. Neurosci. 16 (1996) 4059–4068.
[52] E. Munetsuna, Y. Hojo, M. Hattori, H. Ishii, S. Kawato, A. Ishida, S.A. Kominami, T. Yamazaki, Endocrinology 150 (2009) 4260–4269.
[53] C. Leranth, O. Petnehazy, N.J. MacLusky, J. Neurosci. 23 (2003) 1588–1592.
[54] C. Leranth, T. Hajszan, N.J. MacLusky, J. Neurosci. 24 (2004) 495–499.
[55] Y. Hatanaka, H. Mukai, K. Mitsuhashi, Y. Hojo, G. Murakami, Y. Komatsuzaki, R. Sato, S. Kawato, Biochem. Biophys. Res. Commun. 381 (2009) 728–732.
[57] M.I. Boulware, P.G. Mermelstein, Drug News Perspect. 18 (2005) 631–637.
[58] M.I. Boulware, H. Kordasiewicz, P.G. Mermelstein, J. Neurosci. 27 (2007) 9941–9950.
[59] M.I. Boulware, P.G. Mermelstein, Steroids 74 (2009) 608–613.
[60] Q. Gu, K.S. Korach, R.L. Moss, Endocrinology 140 (1999) 660–666.
[61] J.F. Couse, S.W. Curtis, T.F. Washburn, J. Lindzey, T.S. Golding, D.B. Lubahn, O. Smithies, K.S. Korach, Mol. Endocrinol. 9 (1995) 1441–1454.
[62] M. Kos, S. Denger, G. Reid, K.S. Korach, F. Gannon, J. Mol. Endocrinol. 29 (2002) 281–286.
[63] C. Pendaries, B. Darblade, P. Rochaix, A. Krust, P. Chambon, K.S. Korach, F. Bayard, J.F. Arnal, Proc. Natl. Acad. Sci. U.S.A. 99 (2002) 2205–2210.
[64] S. Dupont, A. Krust, A. Gansmuller, A. Dierich, P. Chambon, M. Mark, Development 127 (2000) 4277–4291.
[65] A. Pedram, M. Razandi, E.R. Levin, Mol. Endocrinol. 20 (2006) 1996–2009.
[66] M. Razandi, A. Pedram, G.L. Greene, E.R. Levin, Mol. Endocrinol. 13 (1999) 307–319.
[68] T.A. Milner, K. Ayoola, C.T. Drake, S.P. Herrick, N.E. Tabori, B.S. McEwen, S. Warrier, S.E. Alves, J. Comp. Neurol. 491 (2005) 81–95.
[69] P. Thomas, Y. Pang, E.J. Filardo, J. Dong, Endocrinology 146 (2005) 624–632.
[70] C.M. Revankar, D.F. Cimino, L.A. Sklar, J.B. Arterburn, E.R. Prossnitz, Science 307 (2005) 1625–1630.
[71] E. Brailoiu, S.L. Dun, G.C. Brailoiu, K. Mizuo, L.A. Sklar, T.I. Oprea, E.R. Prossnitz, N.J. Dun, J. Endocrinol. 193 (2007) 311–321.
[72] E.E. Baulieu, P. Robel, Proc. Natl. Acad. Sci. U.S.A. 95 (1998) 4089–4091.
[73] G. Murakami, N. Tanabe, H.T. Ishii, M. Ogiue-Ikeda, T. Tsurugizawa, H. Mukai, Y. Hojo, N. Takata, A. Furukawa, T. Kimoto, S. Kawato, Drug Metab. Rev. 38 (2006) 353–369.
[74] L. Fester, V. Ribeiro-Gouveia, J. Prange-Kiel, C. von Schassen, M. Bottner, H. Jarry, G.M. Rune, J. Neurochem. 97 (2006) 1136–1144.
[75] J. Prange-Kiel, L. Fester, L. Zhou, H. Lauke, J. Carretero, G.M. Rune, Hippocampus 16 (2006) 464–471.
[76] S. Higo, Y. Hojo, H. Ishii, T. Kominami, K. Nakajima, D. Poirier, T. Kimoto, S. Kawato, Biochem. Biophys. Res. Commun. 385 (2009) 62–66.
[78] Y. Hojo, S. Higo, H. Ishii, Y. Ooishi, H. Mukai, G. Murakami, T. Kominami, T. Kimoto, S. Honma, D. Poirier, S. Kawato, Endocrinology 150 (2009) 5106–5112.
[79] S.H. Mellon, C.F. Deschepper, Brain Res. 629 (1993) 283–292.
[80] J.L. Sanne, K.E. Krueger, J. Neurochem. 65 (1995) 528–536.
[81] A. Furukawa, A. Miyatake, T. Ohnishi, Y. Ichikawa, J. Neurochem. 71 (1998) 2231–2238.
[82] S.L. King, M.J. Marks, S.R. Grady, B.J. Caldarone, A.O. Koren, A.G. Mukhin, A.C. Collins, M.R. Picciotto, J. Neurosci. 23 (2003) 3837–3843.
[83] C. Ibanez, R. Guennoun, P. Liere, B. Eychenne, A. Pianos, M. El-Etr, E.E. Baulieu, M. Schumacher, Endocrinology 144 (2003) 2902–2911.
[84] T. Ivanova, C. Beyer, Cell Tissue Res. 300 (2000) 231–237.
[85] U. Wehrenberg, J. Prange-Kiel, G.M. Rune, J. Neurochem. 76 (2001) 1879–1886.
[86] S. Beyenburg, M. Watzka, I. Blumcke, J. Schramm, F. Bidlingmaier, C.E. Elger, B. Stoffel-Wagner, Epilepsy Res. 41 (2000) 83–91.
[87] R.C. Agis-Balboa, G. Pinna, A. Zhubi, E. Maloku, M. Veldic, E. Costa, A. Guidotti, Proc. Natl. Acad. Sci. U.S.A. 103 (2006) 14602–14607.
[88] T. Kimoto, H. Ishii, S. Higo, Y. Hojo, S. Kawato, Endocrinology 151 (2010) 5795–5806.
[89] T. Higashi, H. Sugitani, T. Yagi, K. Shimada, Biol. Pharm. Bull. 26 (2003) 709–711.
[90] S. Liu, J. Sjovall, W.J. Griffiths, Anal. Chem. 75 (2003) 5835–5846.
[91] P. Liere, A. Pianos, B. Eychenne, A. Cambourg, S. Liu, W. Griffiths, M. Schumacher, J. Sjovall, E.E. Baulieu, J. Lipid Res. 45 (2004) 2287–2302.
[92] E.E. Baulieu, Recent Prog. Horm. Res. 52 (1997) 1–32.
[93] C. Corpechot, P. Robel, M. Axelson, J. Sjovall, E.E. Baulieu, Proc. Natl. Acad. Sci. U.S.A. 78 (1981) 4704–4707.
[94] P. Liere, Y. Akwa, S. Weill-Engerer, B. Eychenne, A. Pianos, P. Robel, J. Sjovall, M. Schumacher, E.E. Baulieu, J. Chromatogr. B: Biomed. Sci. Appl. 739 (2000) 301–312.
[95] F.S. Wu, T.T. Gibbs, D.H. Farb, Mol. Pharmacol. 40 (1991) 333–336.
[96] M. Vallee, W. Mayo, M. Darnaudery, C. Corpechot, J. Young, M. Koehl, M. Le Moal, E.E. Baulieu, P. Robel, H. Simon, Proc. Natl. Acad. Sci. U.S.A. 94 (1997) 14865–14870.
[97] M.J. Ebner, D.I. Corol, H. Havlikova, J.W. Honour, J.P. Fry, Endocrinology 147 (2006) 179–190.
[98] D. Caruso, M. Pesaresi, O. Maschi, S. Giatti, L.M. Garcia-Segura, R.C. Melcangi, J. Neuroendocrinol. 22 (2010) 1137–1147.
[99] K. Yamashita, M. Okuyama, Y. Watanabe, S. Honma, S. Kobayashi, M. Numazawa, Steroids 72 (2007) 819–827.
[100] A.T. Konkle, M.M. McCarthy, Endocrinology 152 (2011) 223–235.

[101] J. Prange-Kiel, H. Jarry, M. Schoen, P. Kohlmann, C. Lohse, L. Zhou, G.M. Rune, J. Cell Biol. 180 (2008) 417–426.

[102] M. Cyr, O. Ghribi, T. Di Paolo, J. Neuroendocrinol. 12 (2000) 445–452.

[103] M. Cyr, O. Ghribi, C. Thibault, M. Morissette, M. Landry, T. Di Paolo, Brain Res. Brain Res. Rev. 37 (2001) 153–161.

[104] C.D. Toran-Allerand, M. Singh, G. Setalo Jr., Front. Neuroendocrinol. 20 (1999) 97–121.

[105] P. Mendez, F. Wandosell, L.M. Garcia-Segura, Front. Neuroendocrinol. 27 (2006) 391–403.

[106] S.M. Belcher, A. Zsarnovszky, J. Pharmacol. Exp. Ther. 299 (2001) 408–414.

[107] E.R. Kandel, J.H. Schwartz, T.M. Jessel, Principles of Neural Science, 4th edition, McGraw-Hill, 2000.

[108] P. Cardona-Gomez, M. Perez, J. Avila, L.M. Garcia-Segura, F. Wandosell, Mol. Cell. Neurosci. 25 (2004) 363–373.

[109] A. Takashima, J. Alzheimers Dis. 9 (2006) 309–317.

[110] P.J. Meberg, W.R. Kinney, E.G. Valcourt, A. Routtenberg, Brain Res. Mol. Brain Res. 38 (1996) 179–190.

[111] J. Balthazart, G.F. Ball, Trends Neurosci. 23 (2000) 57–58.